

III

**ELECTRODEPOSITION OF
Sr-Ti ALLOYED FILMS FROM
AQUEOUS BATH**

CHAPTER-III

ELECTRODEPOSITION OF Sr-Ti ALLOYED FILMS FROM AQUEOUS BATH.

- 3.1 Introduction.
 - 3.2 Experimental Procedure.
 - 3.2.1 FTO Coating On Glass Substrate.
 - 3.2.2 Cleaning Of The Substrates.
 - 3.3 Results And Discussions.
 - 3.3.1 Polarization Curves And Estimation Of Deposition Potentials.
 - 3.3.2 Studies On Growth Parameters Of The Films.
 - 3.3.2.1 Current Density.
 - 3.3.2.2 Aging Effect.
 - 3.3.2.3 Effect Of Temperature On Electrodeposits.
 - 3.3.2.4 Thickness Of The Alloyed Films.
 - 3.4 Oxidation.
 - 3.4.1 Appearance Of The Deposit.
 - 3.5 Microstructures.
 - 3.6 X-Ray Diffraction.
- References.

3.1 INTRODUCTION

Maintaining today's technological advances requires new methods of synthesis of high temperature superconductors(1-5) and their substrates. Recently in most of the studies, efforts have been made to synthesis high temperature superconductors on metallic substrates by using barrier layers, such as SiO_2 on Ag substrates Y-ZrO_2 on stainless steel(6,7).

SrTiO_3 has been found as a suitable substrate for HTc superconductors and HTc superconducting electronic devices, which are prepared by single crystal method or sintering processes(8,9).

Brenner(10) and Messner and Glance(11) have mentioned that electrodeposition of Ti from aqueous bath is not possible due to its high charge to atomic radius ratio. Flinak(12) have reported electrodeposition of Ti

from Flinak melt bath and from chloride electrolyte bath. Strontium, the alkaline earth metal which is electro inactive has extremely negative reduction potential $-3.3V$ vs Ag/Ag^+ (13) restricts some aprotic solvents to be used. Electrodeposition of Sr^{+2} from aqueous bath with proper reagent has been reported by H.J. Hung(14). From survey it is seen that electrodeposition of titanium and strontium from pure aqueous baths are not possible.

The electrodeposition of strontium-titanium alloy may be possible from aqueous bath, if the alloy deposition potential lies below the decomposition potential of water into oxygen and hydrogen.

In this chapter, we report on the electrodeposition of Sr-Ti alloy from an aqueous bath on to copper, brass stainless steel and FTO coated glass substrates. The different preparative parameters were studied and optimised. Alloyed films were oxidised at higher temperatures, in order to obtain the oxide films. The x-ray diffraction pattern and microstructural properties of the films were also studied. ✓

3.2 EXPERIMENTAL PROCEDURE

The electrodepositions were taken with d.c potentiostatic conditions using potentiostat/galvanostat model 362 (EG and G). Three electrode system was

employed and the potentials were measured with respect to saturated calomel electrode (SCE). The electrolysis was accomplished potentiostatically in a 50ml cell. The three electrodes of the electrolytic cell, working electrode (cathode), referene electrode (saturated calomel electrode) and graphit (anode) was connected directly to the scanning potentiostat with the clips provided with the scanning potentiostat. The polarization curves were recorded with a potentiostat and X-Y recorder.

The electrolytic baths were prepared using reagent grade nitrate of strontium and titanium chloride in doubly distilled water. Concentration of Sr-nitrate and Ti-chloride was 100mM and 60mM respectively. These concentrations were decided by optimising for deposition of individual deposits. The bath composition was varied and optimised to be 20:80 percent for Sr-Ti. The pH of the deposition bath was in between 2 and 4.

The electrodeposition was carried out potentiostatically onto stainless steel, copper, brass and (FTO) flourine doped tin oxide coated glass substrates with sheet resistance $20-30\ \Omega/\text{cm}^2$. The substrates were mirror polished. FTO coating was given by spray pyrolysis technique. The backside of the substrate was covered with insulating tape or epoxy resin. The cathode area was 1cm^2 . The distance between the anode and cathode was 0.5cm. The deposited films

were taken out of the bath washed with double distilled water and dried.

All depositions were carried out in an unstirred conditions and at the ambient temperature (300K). In our experiments, quantity of the solution, current range and all other parameters except potentials of the deposition were kept constant.

A DC multimeter was connected in series with the potentiostat, in order to measure the fractions of current changes during deposition. Microstructural properties of the films deposited onto FTO coated glass were carried out with an optical microscope.

A microcomputer controlled phillips diffractometer with CuK_α radiation was used to obtain x-ray diffraction patterns of Sr-Ti alloy as deposited and oxidised films.

3.2.1 FTO COATING ON GLASS SUBSTRATE

Glass substrates were made conducting by giving FTO coating onto these substrates. FTO coating were given by spray pyrolysis technique. Fluorine doped tin oxide (FTO) solution was prepared using A-R grade stannic chloride ($\text{SnCl}_4, 5\text{H}_2\text{O}$), Ammonium flouride (NH_4F) and isoprophyl alcohol $(\text{CH}_3)_2\text{CHOH}$. 100cc of 2M stannic chloride solution was prepared in double distilled water

and 14.285 gms of ammonium fluoride was dissolved in it, to obtain 40% doping concentration of fluorine. From the above mixture 5cc of solution was taken and 20cc of isopropyl alcohol was added. The final solution was sprayed through the specially designed glass nozzle at the spray rate of $6\text{cm}^3/\text{min}$. The substrate temperature was maintained at 550°C . It was found that these conducting glasses have $20\text{-}30\ \Omega/\text{cm}^2$ sheet resistance and about 90% of transparency.

3.2.2 CLEANING OF THE SUBSTRATE

Substrates were cleaned thoroughly before taking the deposition. Cleaning the substrates means breaking down the bonding between the common contaminants such as grease, adsorbed water, air borne dust, lint and oil particles with the substrate material. The technique to be adapted for cleaning depends upon the nature of the substrate, degree of cleanliness and nature of contaminants to be removed.

Thin rectangular substrates were cut according to the desired size and mirror polished. Then they were ordered first from grease by dipping it in a hot and strong 20% alcoholic caustic soda solution for a while and then washed with water. It was next immersed in a moderately strong nitric acid solution containing very little concentrated sulphuric acid. This removes surface scales. It was then washed with sodium carbonate

and again dipped in a slightly acidic solution to remove the alkali adhering to the plate. This is done because acids are easier to wash off than alkalies which adhere to the plate and have pronounced chemical action on the metal. Then the metals were thoroughly washed with alcohol or acetone and then dried well and used as a cathode.

The conducting glass substrates were first washed with the detergent solution and then with the double distilled water. The substrates were boiled in chromic acid for few minutes. After that each substrate is cleaned with distilled water separately. Then sodium hydroxide treatment is given to these substrates. Again the substrates were washed with double distilled water and boiled in double distilled water for some time. Lastly substrates were ultrasonically cleaned. Drying of the substrates is done in the vapour of alcohol with the help of special stand kept in a steel box which will be heated for few minutes.

3.3 RESULTS AND DISCUSSION

3.3.1 POLARIZATION CURVES AND ESTIMATION OF DEPOSITION POTENTIALS

✓ Electrodeposition potential, film morphology and composition of the film depend on the nature of the

substrate. The evolution of Hydrogen at the cathode during the deposition causes the distortion in the crystal structure of the deposits of metals and alloys.

In the present investigation, four different substrates, namely stainless steel, copper, brass and FTO coated glass were electroplated from strontium nitrate, titanium chloride and strontium nitrate-titanium chloride complex baths separately. We have found experimentally the electrodeposition polarization curves of Sr, Ti and Sr-Ti alloy onto different substrates. The polarization curves are shown in figure 1, 2 and 3 respectively.

From the figures, it is seen that, the nature of the polarization curves for stainless steel, copper and brass are similar and the electrodepositions were occurred towards the lower negative potential regions. However, a broad diffused nature of curves is obtained for FTO coated glass substrates. From these polarization curves we have estimated the deposition potentials of Sr, Ti and Sr-Ti alloy and the values of set deposition potentials are listed in Table-I. It is found that, the values of deposition potential depends on the nature of the substrate as the work function changes according to the substrate material.

From the cathodic polarization curves for strontium, decomposition, potential starts from $-0.7V$ vs

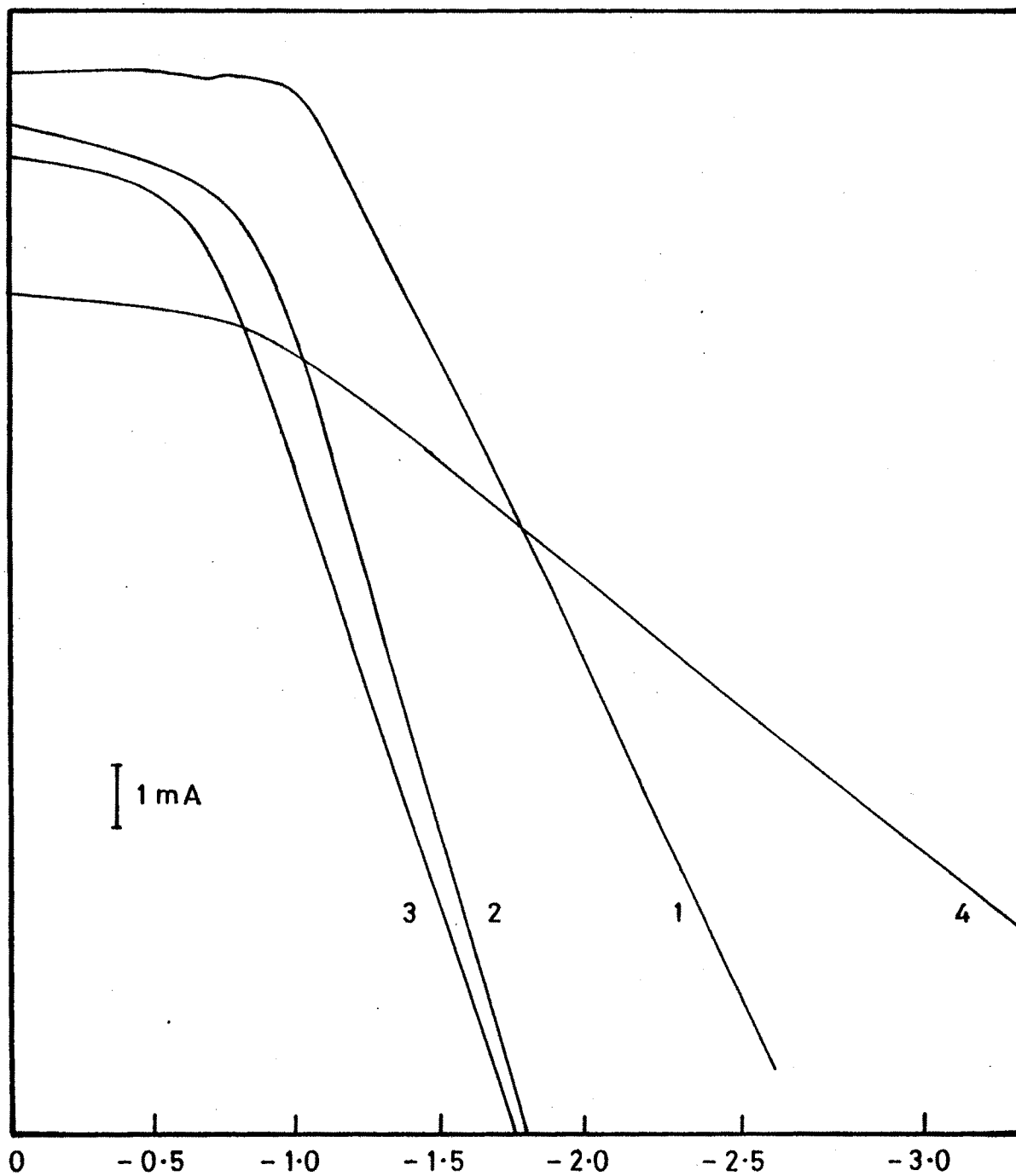


FIG. 1 - POLARIZATION CURVES OF STRONTIUM NITRATE ONTO (1) ST. STEEL (2) BRASS (3) COPPER (4) FTO COATED GLASS.

(SCE) for copper but actual deposition was observed at -1.6V vs (SCE). For brass decomposition potential starts from -0.8V vs (SCE) with deposition taking place at -1.62V vs (SCE). For stainless steel decomposition starts at -1.3V vs (SCE) and deposition was observed at -1.55V vs (SCE). Above the deposition potentials, the increase in current is very high for all these three substrates. For conducting glass substrates, decomposition potential commences from -1.4V vs (SCE) with deposition taking place at -1.8V vs (SCE). For conducting glass, increase in current with applied negative potential is linear. Current ranges for metallic substrates are in $10\text{mA}/\text{cm}^2$ to $40\text{mA}/\text{cm}^2$. For conducting glass substrates they are within $1\text{mA}/\text{cm}^2$ to $5\text{mA}/\text{cm}^2$.

From cathodic polarization curves for titanium, it is clear that residual current is very small for copper and brass substrates, and decomposition potential commences from -0.5V vs (SCE). For stainless steel substrate, decomposition potential commences from -0.6V vs (SCE). For all these three substrates, increase in current is very high above decomposition potential. For conducting glass substrate the nature of the curve is different showing residual current linearly increasing with applied potential from beginning. Deposition potential was experimentally found at -1.5V vs (SCE). Current ranges were within $10\text{mA}/\text{cm}^2$ to

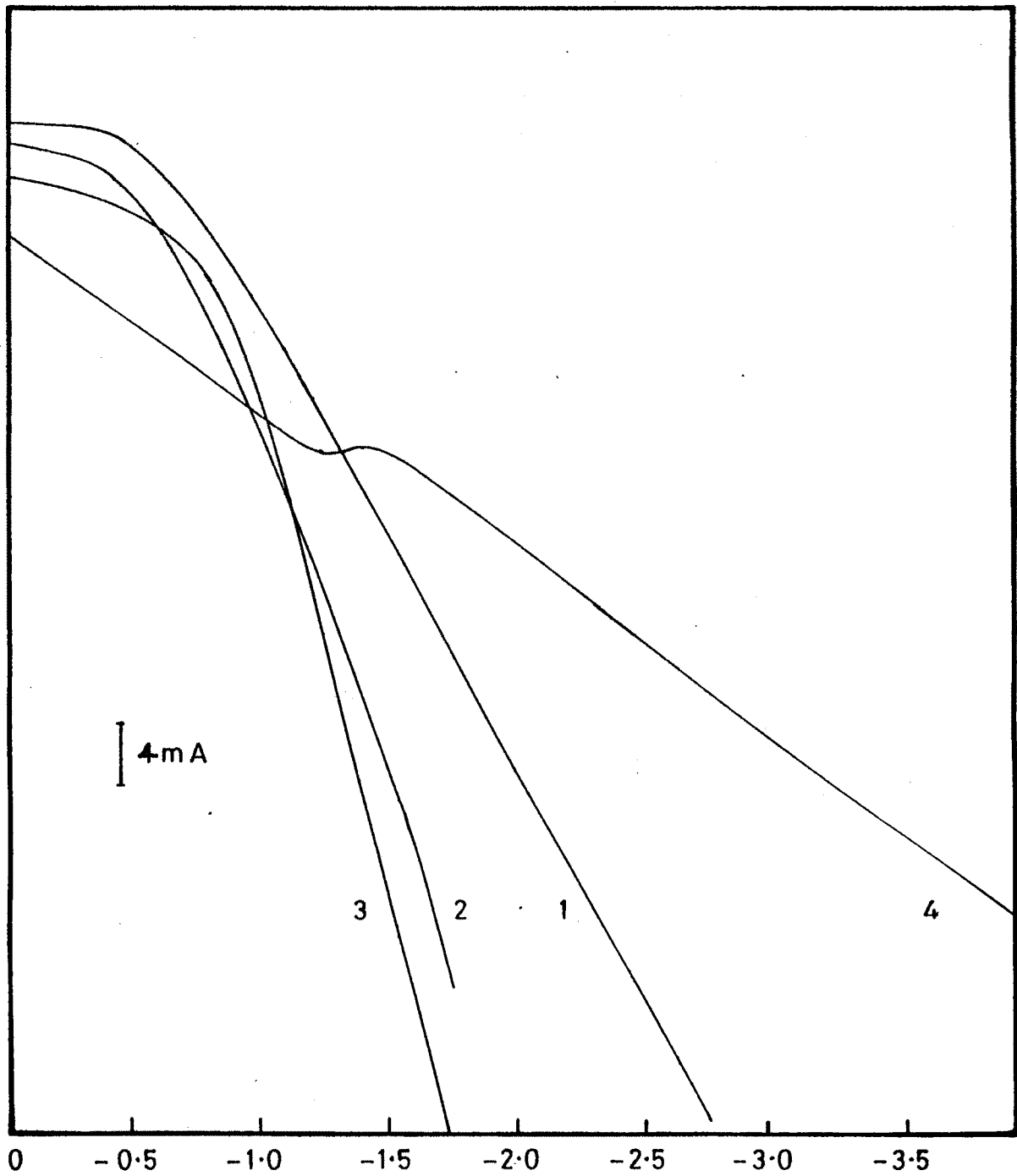


FIG. 2 - POLARIZATION CURVES OF TITANIUM CHLORIDE ONTO (1) ST. STEEL (2) BRASS (3) COPPER (4) FTO COATED GLASS.

30mA/cm² for metallic substrates and for conducting glass substrates within 1mA/cm² to 5mA/cm².

Figure 3 gives the polarization curves of Sr-Ti alloy onto different substrates. For copper substrates residual current is observed from beginning with decomposition potential commencing from -0.3V vs (SCE). Deposition of alloy was observed at -0.89V vs (SCE). For brass decomposition potential was observed at -0.3V vs (SCE) with deposition taking place at -0.85V vs (SCE). For stainless steel substrate decomposition potential was observed at -0.5V vs (SCE), with deposition taking place at -1V vs (SCE).

Deposition potential range was selected from the polarization curve, from -0.6V vs (SCE) to -1.2V vs (SCE), for optimizing the deposition potential for uniform deposition of Sr-Ti alloy. From the studies, it was found at -1V vs (SCE) for stainless steel. For FTO coated glass substrate decomposition potential commences from -1V vs (SCE) with deposition taking place at -2V vs (SCE). Current ranges were 10mA/cm² to 25mA/cm² for metallic substrates and for FTO coated glass substrates they were from 1mA/cm² to 5mA/cm².

From the polarization curves it is seen that at any given potential, the current for Ti⁺⁴ solution baths is higher than Sr⁺² solution bath. This can be understood as follows. The current flowing through the

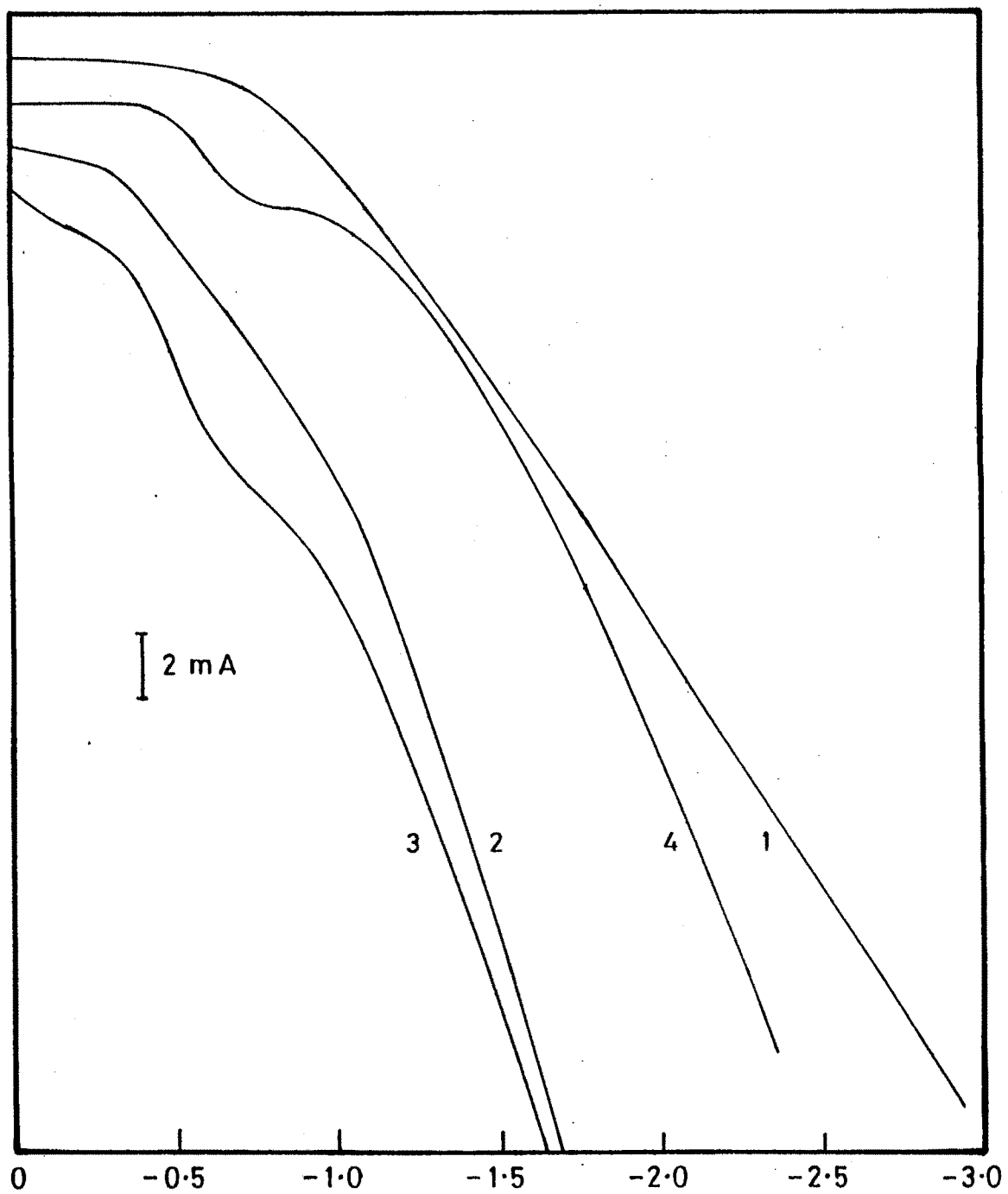


FIG. 3 — POLARIZATION CURVES OF Sr-Ti ALLOY ONTO
(1) ST. STEEL (2) BRASS (3) COPPER
(4) FTO COATED GLASS .

electrodeposition cell is consisted of the electronic current and the ionic current. Current through electrodeposition cell is given by the relation,

$$I_{E^c} = N.Z \frac{u}{v} + \text{electronic current} \quad \text{-----} I$$

Where N is the number of positive ions moving to the cathode and getting deposited on the cathode, Z is the valency of the positive ion, u is the velocity of the positive ion and v is the voltage applied to the electrolytic deposition cell. In electrolytic deposition cell, the contribution due to electronic current is comparatively smaller than the ionic transport current. At a given fixed potential V and at constant temperature T, with the velocity u of the transport ion I_{E^c} is mainly governed by the positive valency of the ion giving rise to the higher value of I for Ti^{+4} solution bath than that of Sr^{+2} solution bath.

However, the values of the electrolytic deposition cell current I for alloyed bath are grater than the values of I for Sr^{+2} and smaller than Ti^{+4} . This may be attributed to the fact that the simultaneous transport of Sr^{+2} and Ti^{+4} ions towards cathode is complex process interlinked to each other giving rise to locking their free ionic motions. Alternatively it may be possible that these two positive ions may form a big complex molecule reducing their transport velocity and hence the current change.

3.3.2 STUDIES ON GROWTH PARAMETERS OF THE FILMS ✓

3.3.2.1 CURRENT DENSITY

Figure 4 shows the variation of deposition current with time at different fixed deposition potentials on stainless steel substrate for Sr-Ti of 20:80 percent composition. From figure it is seen that, the behaviour of current density with time are more or less similar for different fixed deposition potentials. It is observed that, the current density drastically decreases within first five minutes due to the rapid deposition of the alloy layer on the substrate, thereby causing an increase in surface resistance. After the sudden decrease, the current density practically remains constant with longer deposition time. Similar results were obtained for other substrates.

3.3.2.2 AGING EFFECT

We have observed the effect of solution aging (24 hours) on the variation of current densities with time for stainless steel substrate. The main effect observed was increase in current densities with evolution of H_2 at the time of deposition. Depositions were not uniform and dense. For this reason, fresh solutions of Sr-nitrate and Ti-chloride were prepared for the deposition of Sr-Ti alloy.

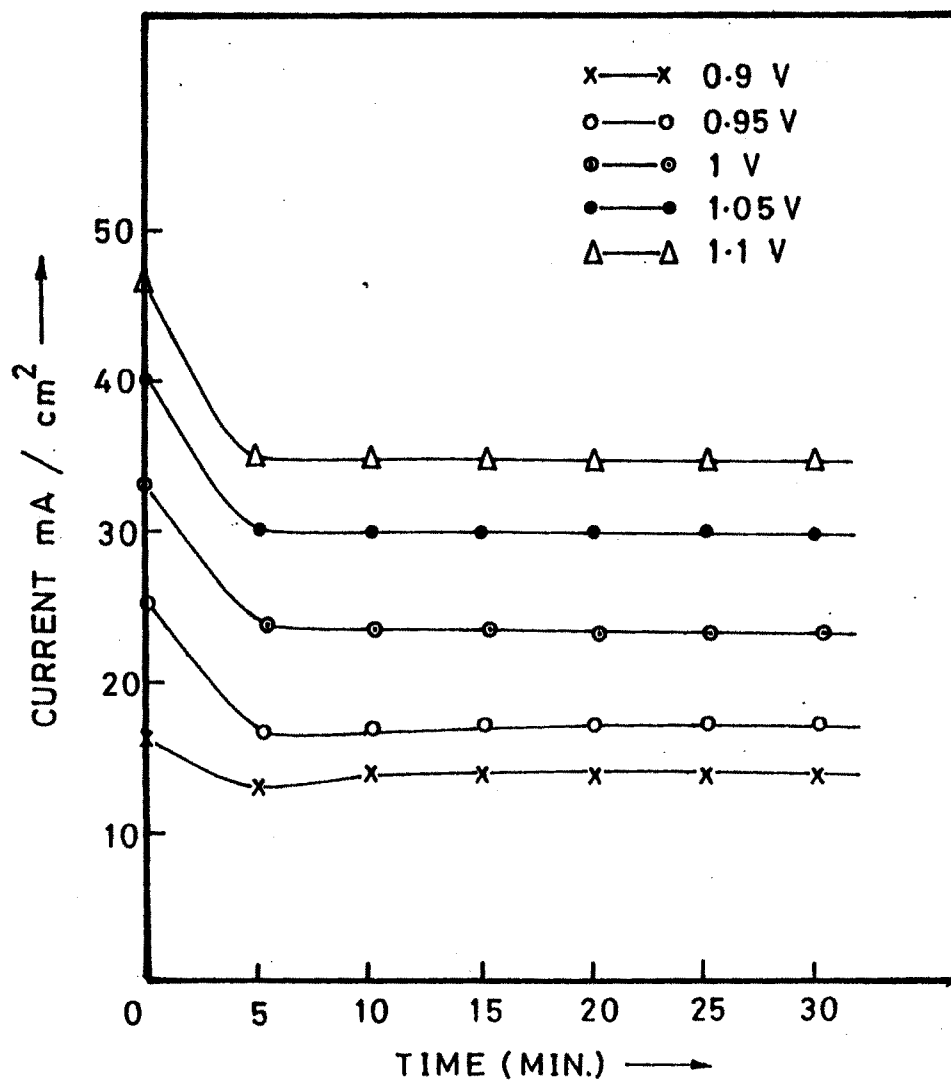


FIG. 4 — VARIATION OF DEPOSITION CURRENT DENSITY WITH TIME FOR DIFFERENT DEPOSITION POTENTIALS.

3.3.2.3 EFFECT OF TEMPERATURE ON ELECTRODEPOSITS

The temperature of the bath can affect electrodeposition in a number of ways. In general, an increase in the temperature increases the rate of diffusion as well as the ionic mobilities and hence the conductivity of the bath. It may influence the dissociation of the complex ion, the current, the diffusion of ions and the over potential at the cathode. At higher temperatures higher current densities are possible and hence, it is possible to produce fine grained and smooth deposits by heating the bath solution. At higher temperature as cathode film is replenished rapidly, tendency towards treeing is reduced.

In our experiment, it is observed that as the temperature of the bath is raised, the current density is increased with the evolution of H_2 and Cl_2 at the cathode and anode respectively, which cause the distortion in the crystal structure of the deposits of metals and alloys. The deposits obtained with aged solutions for more than 24 hours with increase of temperature are found with more pin holes which distructs the uniformity of the thin films.

3.3.2.4 THICKNESS OF THE ALLOYED FILMS

From the voltamogram (polirazation) curves we have selected the range of potential for the study to

find dense, uniform and adhesive electrodeposition, from -0.6V vs (SCE) to -1.2V vs (SCE) . Figure 5 shows the variation of Sr-Ti film thickness with different fixed potentials onto stainless steel substrates. Electrodeposition were carried out at fixed time of 30 minutes. From the figure it is seen that, the Sr-Ti film thickness were continuously increased with the increase in deposition potential.

However, uniform smooth and adhesive films with improved thickness of Sr-Ti alloy were obtained at -1V vs (SCE) . At -1V vs (SCE) potential, we have studied the variation of film thickness with deposition time (figure 6). The Sr-Ti film thickness linearly increases with deposition period of 25 minutes and afterwards very slowly saturates with longer deposition period. The thickness of the Sr-Ti film is of the order of 4 to 5 microns for the deposition period of 30 minutes. This variation of film thickness with time is depicted in figure 6.

Consequently, we have studied the charge passed through the deposition bath as a function of deposition time and the nature of the plot is depicted in figure 7. From the figure, it is observed that thickness of Sr-Ti alloyed film should increase linearly with deposition time. However, thickness of the film very slowly saturates after 25 minutes. This might be

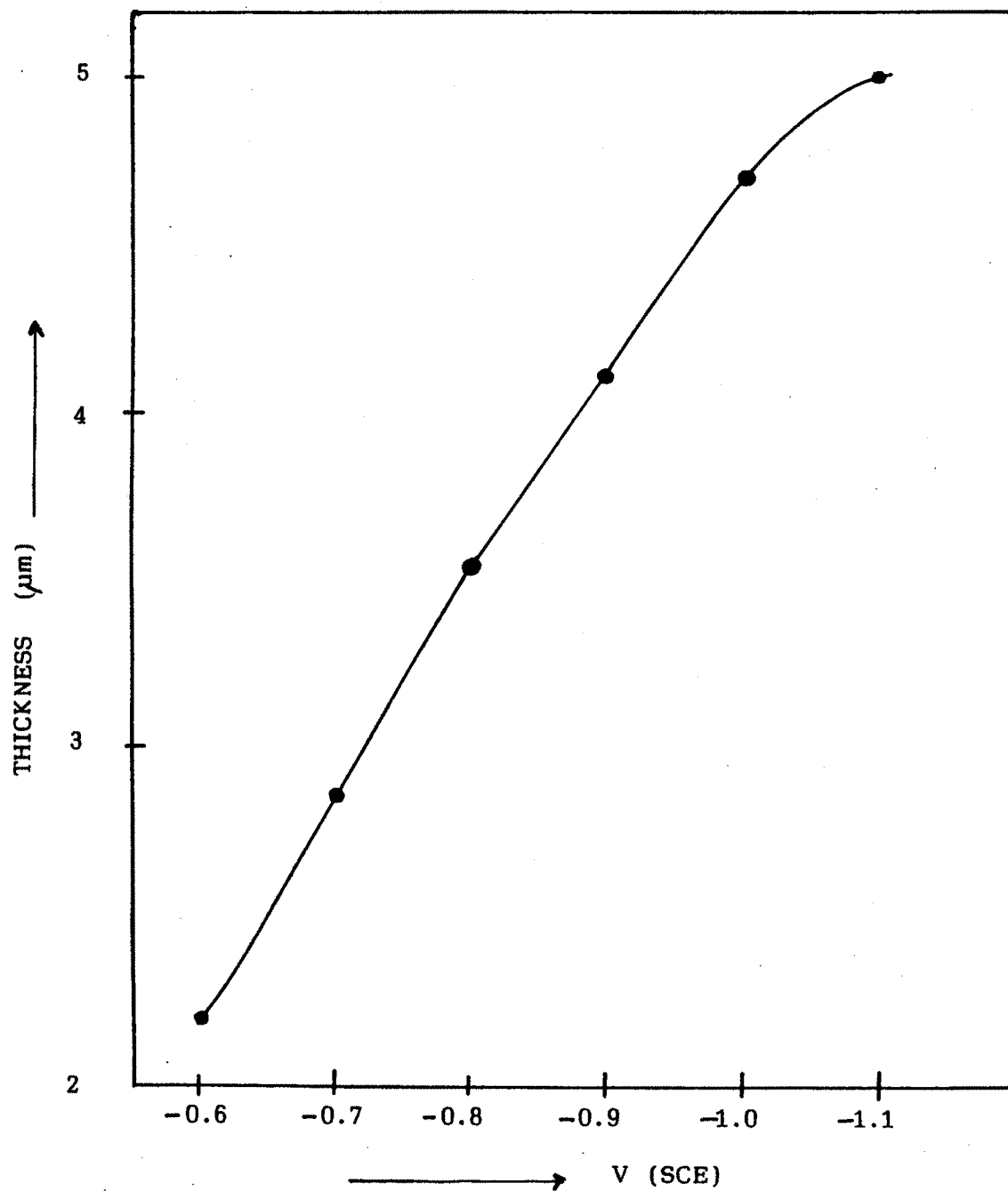
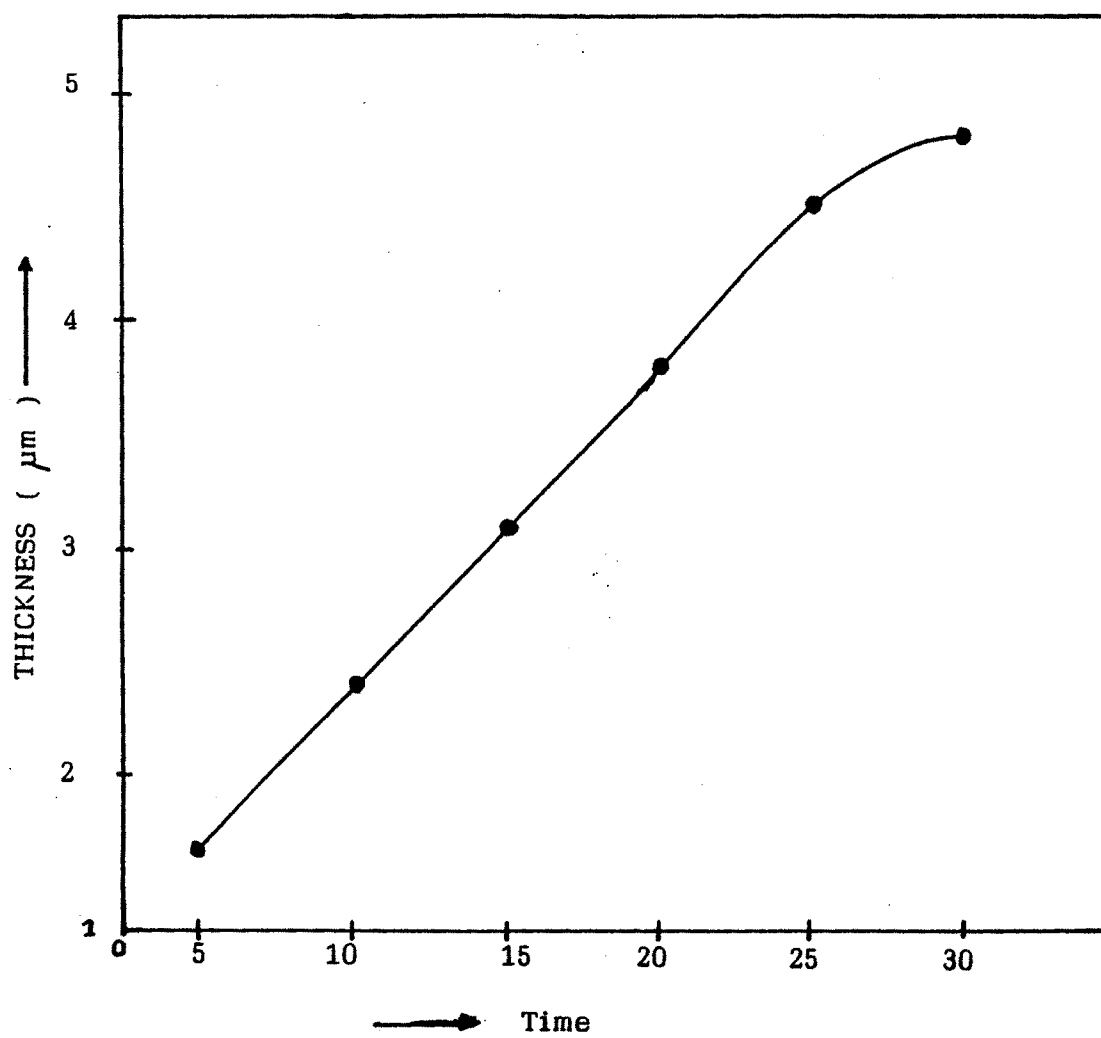


Fig.5 : The variation of Sr-Ti film thickness for 30 minutes of deposition at different deposition potentials.



GRAPH OF THICKNESS Vs TIME

Fig.6 : The variation Sr-Ti film thickness with deposition time in minutes, at potential -1V Vs (SCE)

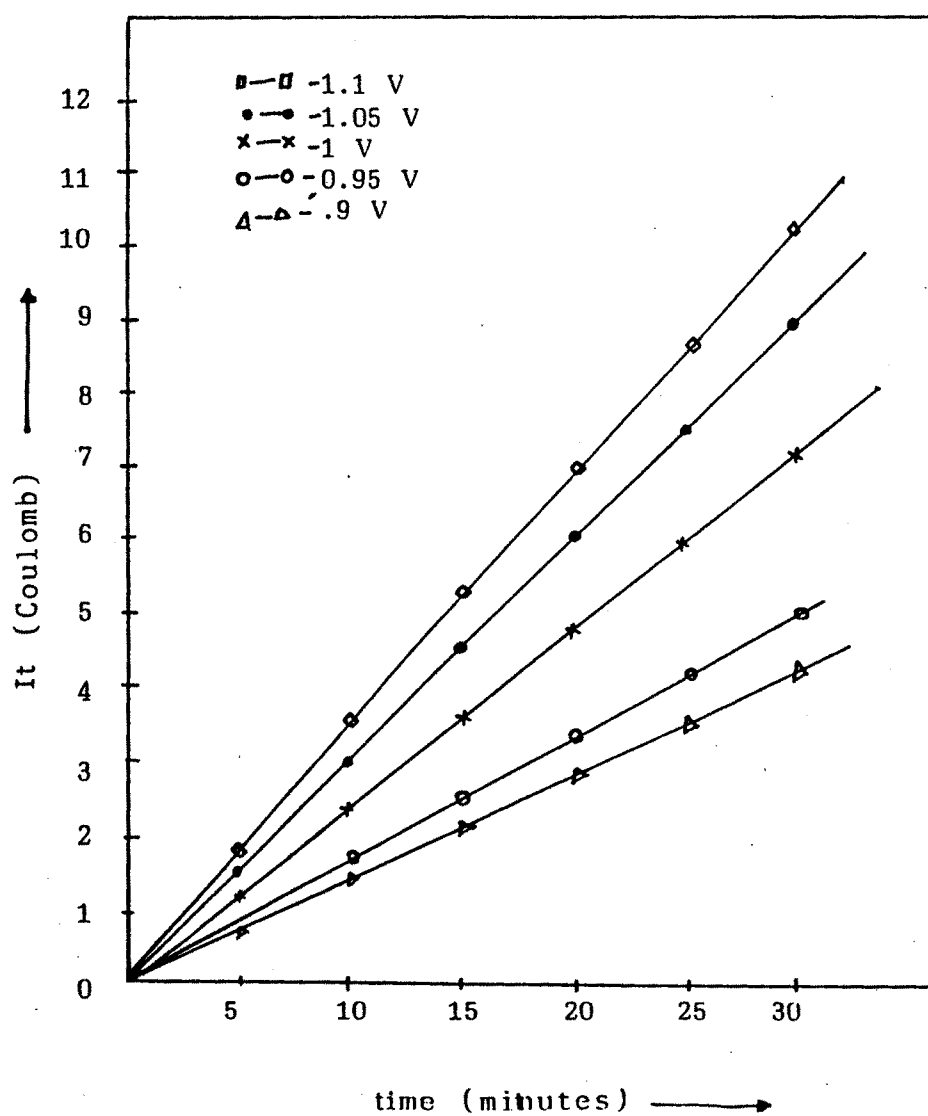


Fig. 7 : The total charge passed through deposition bath with deposition time.

due to the acidic nature of the deposition bath, which causes the very slow dissolution of the film back into the deposition bath.

3.4 OXIDATION

Heating the metal or alloy to an appropriate temperature in a controlled atmosphere is called the direct oxidation. A uniform layer of oxides may be produced in this way.

The direct oxidation of metals and alloys may be considered as tarnish reactions. These are reactions of a solid with a gas or liquid. In case of thick films ($w = 100$ AU) two type of laws are observed (18). In the linear dependence of thickness on time

$$W = A.t \text{ ----- I}$$

is observed, and in the parabolic dependence

$$W^2 = B + C.t \text{ ----- II}$$

is observed where A, B and C are constants.

In the linear relation, the gas reaches the metal surface whereas the parabolic law applies to the growth which is limited by diffusion through a coherent solid film. The parabolic law depends on the properties of the bulk solid. In the reaction of a metal M with a gas X to give MX, following transport phenomena are (19) assumed. Fig A . represents the motion of interstitial

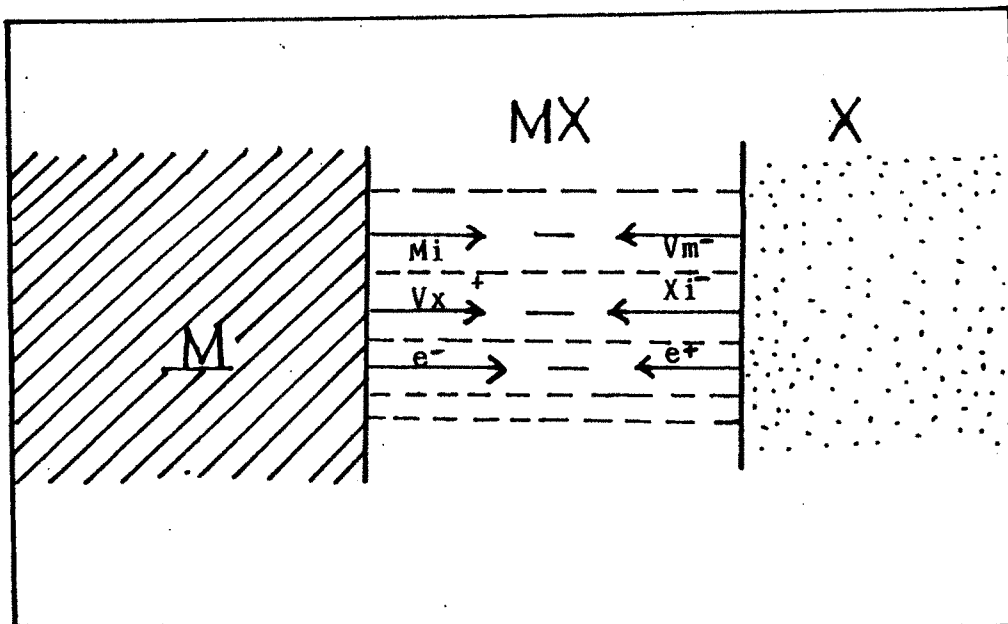


Fig. A : OXIDATION MECHANISM

cations or anions vacancies from I to II or of cation vacancies and interstitial anions from II to I.

3.4.1 APPEARANCE OF THE DEPOSIT

Films deposited onto metallic substrates were smooth, uniform, dense and adhesive to the substrate. The deposits obtained at room temperature from fresh bath of strontium nitrate and titanium chloride were smooth, uniform, dense and adhesive to the substrates. Deposition on conducting glass substrate were also uniform and adhesive to the substrates. The Sr-Ti alloyed deposits were whitish in colour and stable towards the atmospheric conditions.

The Sr-Ti as deposited films were oxidised at higher temperatures in order to obtain the oxide films of SrTiO_3 . Films were air oxidised at 400°C to 10 minutes. The oxidised films were uniform and adhesive to the substrates. The resistance measurement of the oxidised films were recorded and are found in the range of $5\text{M}\Omega$ to $10\text{M}\Omega$ at room temperatures.

3.5 MICROSTRUCTURES

Figures 8(a-c) show surface morphology of typical samples of as deposited Sr, Ti and Sr-Ti alloy. Figure 8d shows the surface morphology of typical sample of Sr-Ti alloy oxidised at 400°C for 10 minutes. The



Fig. 8a : Surface Morphology of as deposited strontium
from strontium nitrate bath



Fig. 8b : Surface Morphology of as deposited titanium
from titanium chloride bath

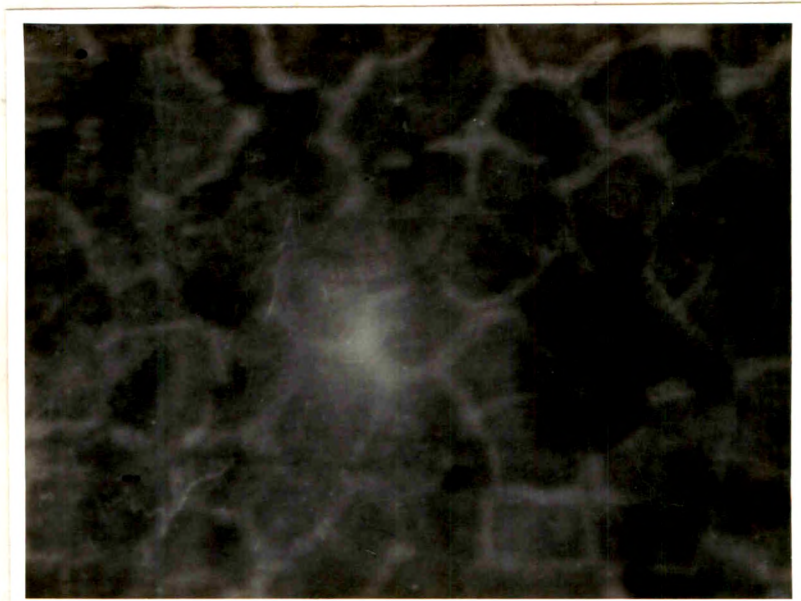


Fig. 8c : Surface Morphology of Sr-Ti alloy as deposited from aqueous bath

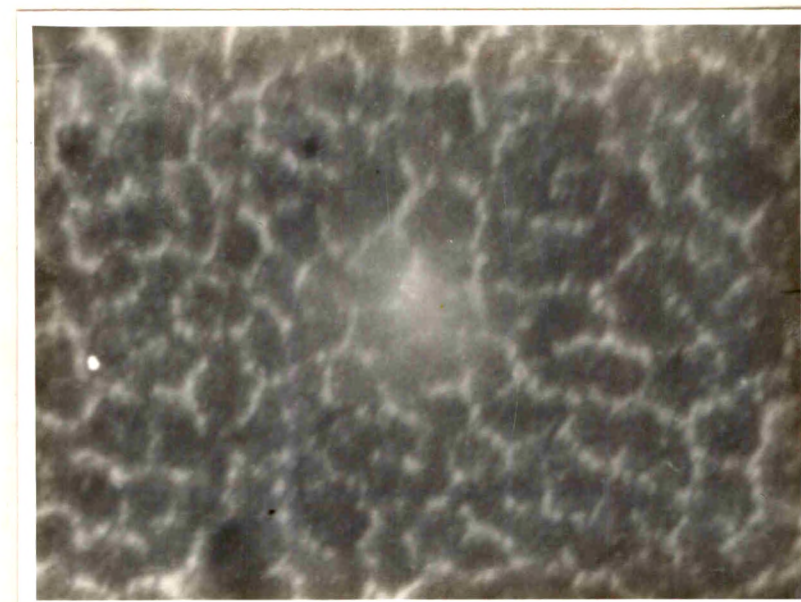


Fig. 8d : Surface Morphology of Sr-Ti alloy oxidised at 400°C for 10 minutes

magnification was 500X. From the micrographs it is observed that, films obtained by the electrodeposition technique are smooth, dense, uniform and having packed arrangements of grains. Fig 8a shows that the Sr films are polycrystalline with grain sizes ranging from $4\mu\text{m}$ to $7\mu\text{m}$ with intergrain boundary spacing ranging from $0.5\mu\text{m}$ to $1.5\mu\text{m}$. Fig 8b shows that the Ti films are polycrystalline with very fine grain size. Fig 8c and Fig 8d show a homogeneous polycrystalline structure. With hexagonal plate-like structure. Grain size is ranging from $3\mu\text{m}$ to $5\mu\text{m}$. After oxidising the alloy samples, coalescence of the grains are observed with decreased intergrain spacing.

3.6 X-RAY DIFFRACTION

X-ray diffraction patterns of Sr-Ti alloy as deposited and oxidised at 400°C were obtained with PW1710 Diffractometer. Figure 9 shows the x-ray diffraction pattern of Sr-Ti alloyed films onto stainless steel substrates. From x-ray diffraction pattern, it is seen that, the electrodeposited films of Sr-Ti are of polycrystalline in nature. However, crystallinity of the film was improved with oxidation. The diffraction pattern shows the face centered cubic pattern of doublets with increased spacing as 2 θ value is increased. Oxidation has increased the first doublet

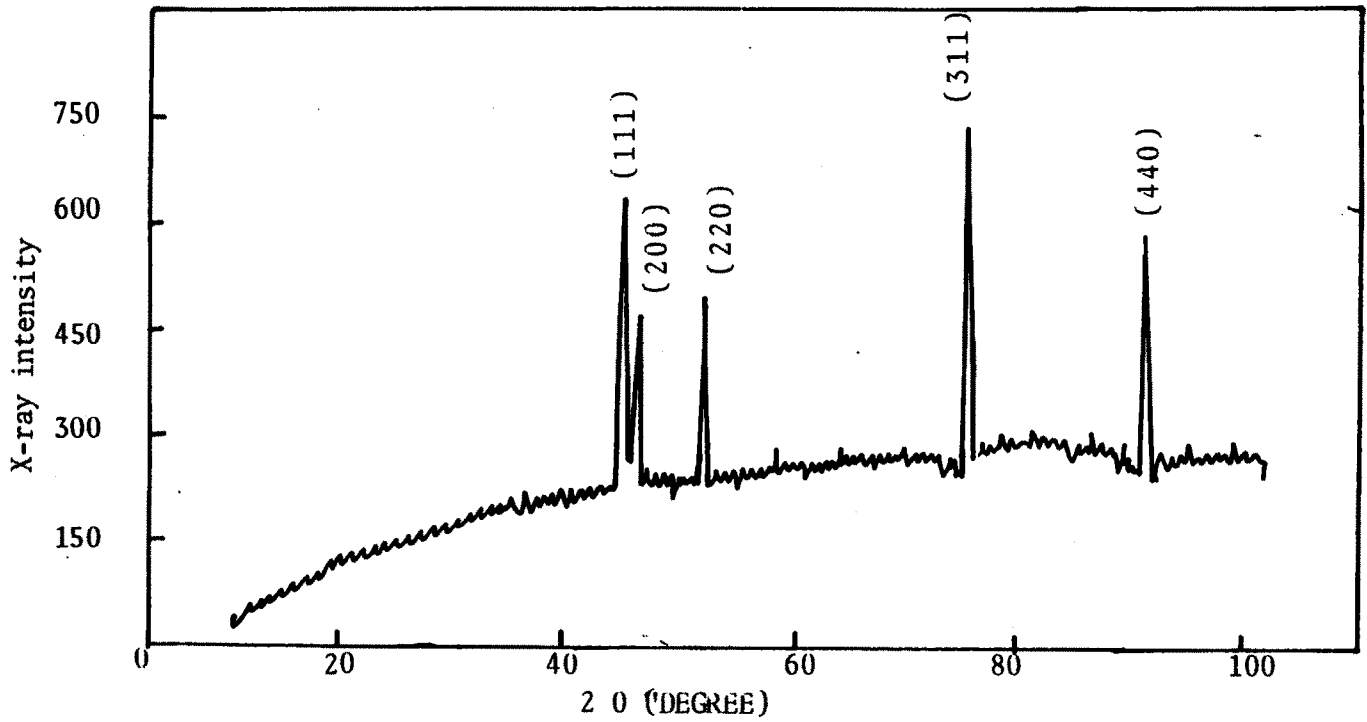


Fig. 9 : X-ray diffraction pattern of electrodeposited Sr-Ti alloyed films as deposited from aqueous bath.

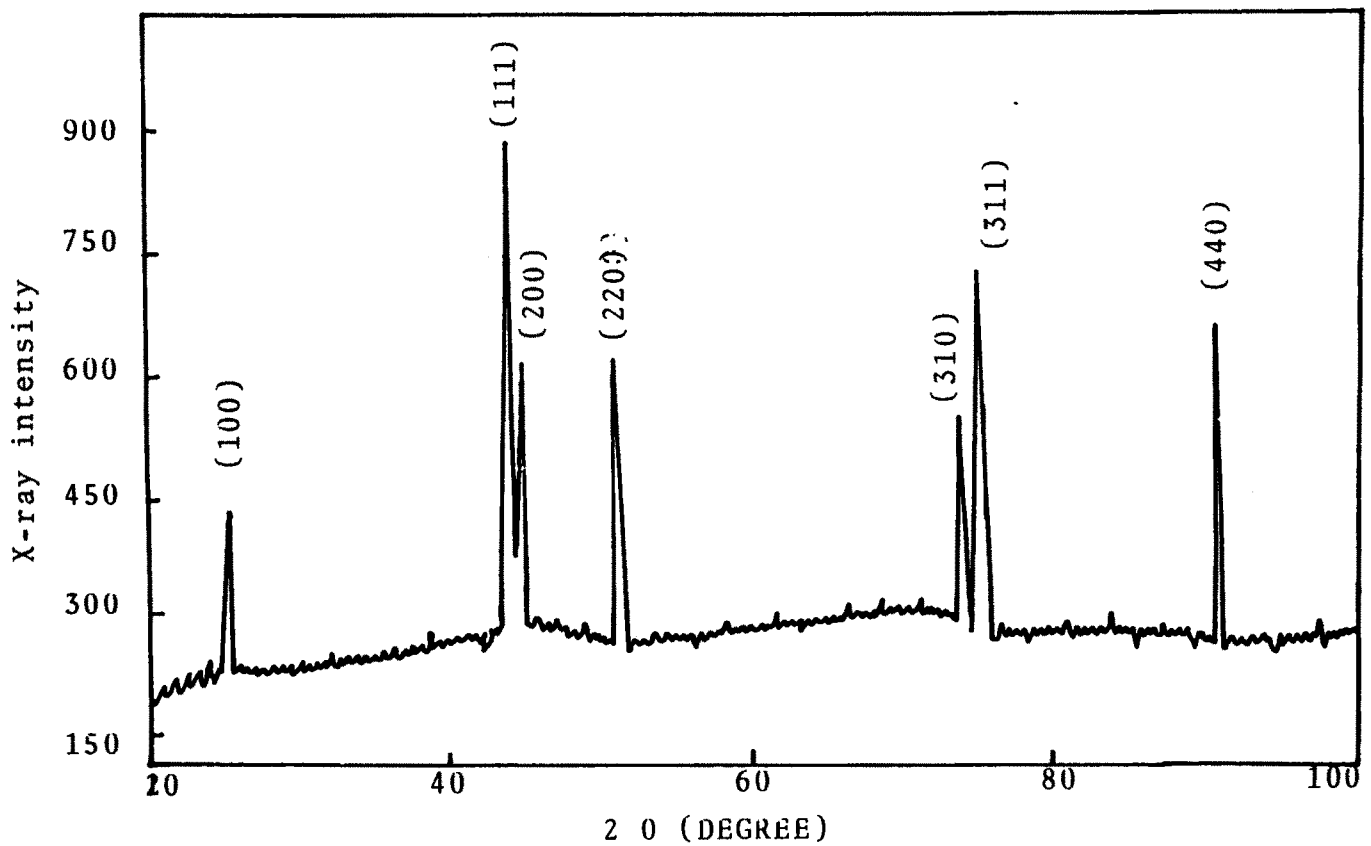


Fig. 9 : X-ray diffraction pattern of Sr-Ti alloy films oxidised at 400°C from aqueous bath.

intensity of (100) peak of SrTiO_3 has been observed in oxidised x-ray diffraction pattern.

Strontium titanate has perovskite crystal structure of ABO_3 form. The structure is cubic, with Sr^{+2} ions at the cubic corners, O^{-2} ion at the face centres and Ti^{+4} ion at the body center. It may be described as a cubic close-packed arrangement of the oxide ions and the larger cations, with the smaller cations occupying octahedral interstices in an ordered pattern. The resulting structure has a cubic unit cell which is shown in figure B.

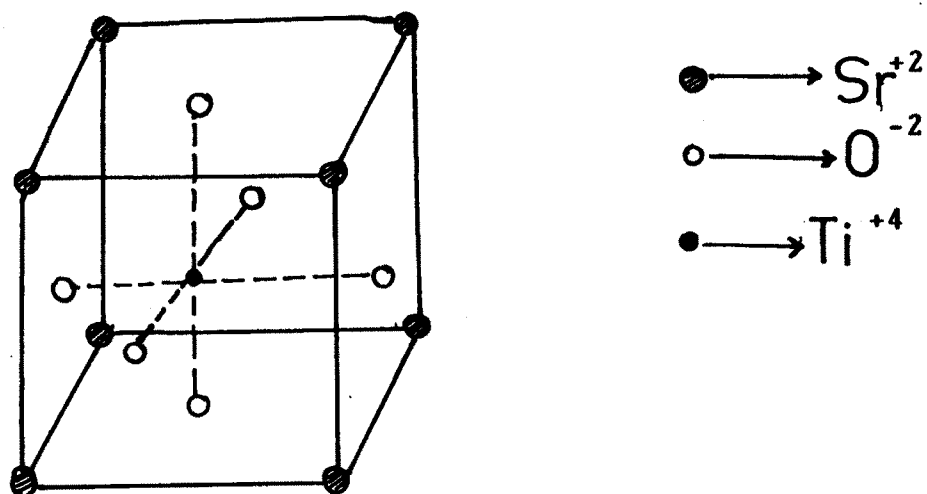


Fig. B : CRYSTAL STRUCTURE

THE PEROVSKITE STRUCTURE

Open circles are O^{-2} ions large shaded circles are the large cation (Sr^{+2}) small shaded circle is Ti^{+4} ion.

Table 1 : The electrodeposition potentials of Sr, Ti and Sr-Ti alloy from their nitrate and chloride solutions onto different substrates

Substrates	Electrodeposition Potentials V vs (SCE)		
	Sr	Ti	Sr-Ti alloy
Stainless steel	-1.55	-0.79	-1.0
Copper	-1.66	-0.70	-0.89
Brass	-1.62	-0.73	-0.85
FTO coated glass	-1.80	-1.50	-2.00

REFERENCES

1. J.G. Bednorz and K.A. Muller, Z Phys. B. 64 189(1986).
2. M.K. Wu, J.R. Ashburn, C.J. Torng, P.H. Hor, R.L. Meng; L.Gao. Z.J. Huang, Y.O Wang and C.W. Chu Phys Rev Lett 58, 908(1988).
3. S. Hatta, H. Higashino, K. Hirochi, H. Adachi, and K.Wasa, Appl Phys Lett 53, 148(1988).
4. T. Asano, K. Tran, A.S. Byrne, M.M Rahaman, C.Y. Hang and J.D. Reardon. Appl, Phys. Lett. 54, 1275(1989).
5. S.B. Ogale, R.D. Vispute, and R.R. Rao. Appl. Phys. Lett 57, 1805 (1990).
6. Akira Yoshida, Hirotaka Tomura, Hideki Takauchi and Shinya Hasuo. Appl. Phys. Lett. 59(10), 2 September (1991) P.1242.
7. S.B. Ogale. V.N. Konikar. R. Viswanathan, S.D. Roy, and S.M. Kanetkar. Appl. Phys. Lett. 59(15), 7 October (1991) P.1908.
8. B.J. Kellett, J.H. James, A. Gauzzi, B. Pavuna, and F.K. Reinhart. Appl. Phys. Lett 57(11), 10 September (1990) P.1146.
9. R. Brown, V. Pendrick, and D. Kalokitis Appl. Phys Lett. 57(13), 24 September (1990) P.1351.

10. A. Brenner. Adv. Electrochem: Electrochem Eng. 5. (1967), 209.
11. Maissel and Glang. Handbook of Thin Film Technology. Electroplating. 5-8 (1970).
12. Flinak. Melts, H. Wendt et al. P. 237 Electrochimica, Acta, Vol. 37, No.2, PP 237-244, (1992).
13. M. Maxheld, H. Eckhardt, Z. Iqbal, F. Reidinger, and R.H. Baughman. Appl. Phys. Lett 54(19), 8 May, (1989), P.1932-33.
14. H.J. Hung. J. Electrochem, Soc. P-630. March (1983).
15. B.N. Popov, M.C. Kimble, R.E. White and H. Wendt. J. Appl, Electrochem. 21, 351 (1991).
16. C.T. Rogers, A. Inam, M.S. Hegde, B. Dutta, X.D. Wu, and T. Venkatesan. Appl. Phys. Lett. 55(19), 6 November (1989). P.2032.
17. S.H. Pawar, B.N. Todkar, H.A. Mujawar and M.H. Pendsa.
18. N.B. Hanney, Solid state chemistry, Printice Hall Inc., P, 161, (1967).
19. W.P. Gomes and W. Dekeyser in Treatise on solid state chemistry Vol.4 Plenum Press P, 76(1976), (N.B. Hannery ed.).

